

Study of cyclohexanol decomposition reaction over the ferros spinels, $A_{1-x}Cu_xFe_2O_4$ ($A = Ni$ or Co and $x = 0, 0.3, 0.5, 0.7$ and 1), prepared by ‘soft’ chemical methods

C.G. Ramankutty^a, S. Sugunan^{b,*}, Bejoy Thomas^b

^a Department of Chemistry, Union Christian College, Aluva 683 102, Kerala, India

^b Department of Applied Chemistry, Cochin University of Science and Technology, Cochin 22, Kerala, India

Received 24 September 2001; accepted 13 March 2002

Abstract

Preparation of simple and mixed ferros spinels of nickel, cobalt and copper and their sulphated analogues by the room temperature coprecipitation method yielded fine particles with high surface areas. Study of the vapour phase decomposition of cyclohexanol at 300 °C over all the ferros spinel systems showed very good conversions yielding cyclohexene by dehydration and/or cyclohexanone by dehydrogenation, as the major products. Sulphation very much enhanced the dehydration activity over all the samples. A good correlation was obtained between the dehydration activities of the simple ferrites and their weak plus medium strength acidities (usually of the Brønsted type) determined independently by the *n*-butylamine adsorption and ammonia-TPD methods. Mixed ferrites containing copper showed a general decrease in acidities and a drastic decrease in dehydration activities. There was no general correlation between the basicity parameters obtained by electron donor studies and the ratio of dehydrogenation to dehydration activities. There was a leap in the dehydrogenation activities in the case of all the ferros spinel samples containing copper. Along with the basic properties, the redox properties of copper ion have been invoked to account for this added activity.

© 2002 Elsevier Science B.V. All rights reserved.

Keywords: Cyclohexanol decomposition; Ferros spinels; Sulphated ferros spinels; Copper containing ferrites; Catalysis by spinels

1. Introduction

Unlike single oxides or their mixtures, the single phase spinel-type binary and ternary oxides show extra structural stability and exhibit interesting catalytic properties. The catalytic activity of spinels containing transition metal ions is influenced by the acid–base and redox properties of these ions as well as by their distribution among the octahedral and tetrahedral sites in the spinel structure. It had been established that the

octahedral sites are almost exclusively exposed at the surface of the spinel crystallites and that the catalytic activity is mainly due to octahedral cations [1,2].

The preparation of spinels by the conventional ceramic methods gave only coarse and inhomogeneous samples with low surface areas. Ever since the first report of their preparation by the ‘soft’ chemical route by Date and coworkers [3], there has been a renewed interest in exploring the catalytic properties of ferros spinels. This new method gives very fine particles with high surface areas and catalytic activity. Such samples were found to be effective for alkylation of aniline [4–6] and phenol [7].

* Corresponding author. Fax: +91-484532495.
E-mail address: ssg@cusat.ac.in (S. Sugunan).

We have been investigating the surface properties and catalytic activity of the ferros spinels of nickel, cobalt and copper, prepared by the low temperature coprecipitation route and their sulphated analogues. The surface properties of these oxides have been evaluated by adopting various physico-chemical methods and the catalytic activity towards the liquid phase Friedel–Crafts benzoylation of toluene has already been reported by us elsewhere [8].

Alcohol decomposition reaction has been widely studied because it is a simple model reaction to determine the functionality of an oxide catalyst, to be chosen for industrial processes. Decomposition of isopropanol and that of cyclohexanol (CHOL) are the most widely studied reactions in this category. Dehydration activity is linked to the acidic property and dehydrogenation activity to the combined effects of both acidic and basic properties of the catalyst. Decomposition of alcohols is one among the many classes of reactions catalysed by oxidic spinels. Studies on the decomposition of isopropanol [9,10], benzyl alcohol [11,12] and CHOL [13,14] by spinel oxides have been reported.

In the present investigation, two series of ferros spinels namely, $\text{Ni}_{1-x}\text{Cu}_x\text{Fe}_2\text{O}_4$ and $\text{Co}_{1-x}\text{Cu}_x\text{Fe}_2\text{O}_4$ ($x = 0, 0.3, 0.5, 0.7$ and 1) and their sulphated analogues have been prepared by the room temperature coprecipitation method. The systems are often subdivided into simple ferros spinels, AFe_2O_4 ($\text{A} = \text{Ni, Co and Cu}$) and mixed ferros spinels of the nickel–copper series and the cobalt–copper series ($x = 0.3, 0.5, 0.7$) for convenience. The surface properties and catalytic activity of these oxides for the vapour phase decomposition of CHOL have been studied at a reaction temperature of 300 °C. Excellent conversions have been found for the reaction at this relatively low reaction temperature to give both cyclohexene and cyclohexanone as the major products. The best yield (70%) of cyclohexanone was given by cobalt–copper ferrite with $x = 0.5$ and the best yield of cyclohexene (65%) by sulphated nickel–copper ferrite with $x = 0.7$. Copper containing ferrites showed very high activities for dehydrogenation and can be recommended as highly promising catalysts for the manufacture of cyclohexanone, the key precursor for nylon-6 and nylon-66. Sulphation of the ferros spinels caused a net increase in their catalytic activities and uniformly enhanced the dehydration activities of all the samples.

2. Experimental

2.1. Preparation and characterisation

The experimental details regarding the preparation of the catalyst samples and the methods of characterisation such as XRD analysis, infrared spectra, energy dispersive X-ray (EDX) analysis, BET surface area, thermogravimetric analysis (TGA) and Mossbauer spectra have been described in our earlier paper [8]. The same is the case with the experimental details of evaluating the Lewis basicity by adsorption of electron acceptors on electron donor (ED) sites of the catalyst and evaluating acidity by adsorption of *n*-butylamine.

2.2. Acidity determination: (a) ammonia-TPD and (b) adsorption of 2,6-dimethylpyridine

For ammonia-TPD (temperature programmed desorption) studies, pelletised catalyst was activated at 300 °C inside the reactor of the TPD furnace under nitrogen flow for half-an-hour. After cooling to room temperature, ammonia was injected in absence of carrier gas flow and the system was allowed to equilibrate. A current of nitrogen flushed out the excess ammonia. The temperature was then raised in a stepwise manner at a linear heating rate of about 20 °C/min. The ammonia desorbed from 100 to 600 °C at intervals of 100 °C was trapped in a known excess of standard dilute sulphuric acid and estimated by back titration with sodium carbonate. The amounts of ammonia desorbed in the temperature values of 100–200, 300–400 and 500–600 °C were taken as measures of weak, medium and strong acid sites.

For 2,6-dimethylpyridine (DMP) adsorption studies, the activated catalysts were kept in a desiccator saturated with DMP vapours at room temperature for 48 h. Then the weight loss of the adsorbed sample was measured by TGA (Mettler Toledo S R) operating between 40 and 600 °C at the heating rate of 20 °C/min. The weight loss between 160–300, 300–440 and 440–580 °C were considered to be measures of weak, medium and strong acid sites, respectively.

2.3. Vapour phase decomposition of CHOL

CHOL from Merck was used as such without further purification. The reaction was done at

atmospheric pressure in a fixed bed, vertical, down-flow, integral silica reactor placed inside a double-zone furnace (Solelem, France). The catalysts were pressed, pelletised and broken into uniform pieces and sieved to obtain catalyst particles of size 10–20 mesh. Exactly 3 g catalyst was charged each time in the centre of the reactor in such a way that the catalyst was sandwiched between the layers of inert porcelain beads. The upper portion of the reactor served as a vapouriser cum pre-heater. All heating and temperature measurements were carried out using 'Aplab' temperature controller and indicator instruments.

A thermocouple was positioned at the centre of the catalyst bed to monitor the exact temperature of the catalyst bed. The catalysts were activated in the reactor itself at 573 K in a sufficient flow of dry air for at least 3 h before each run. The liquid reactant was fed by a syringe pump (ISCO model 500 D). The products of the reaction were collected downstream from the reactor in a receiver connected through a cold water circulating condenser. Products were collected at various time intervals and analysed by gas chromatography (Shimadzu, model 15A, HP ultra capillary column, FID detector, N₂ carrier gas, injection port temperature 250 °C, column temperature 80 °C, detector temperature 250 °C). Identification of products was done by comparing the GC retention times of expected products with those of standard samples.

3. Results and discussion

3.1. Characterisation by physical methods

3.1.1. XRD analysis

The experimental XRD data of the simple ferrites agreed very closely with the standard values given in the JCPDS Data Cards, thus confirming the inverse spinel structure. The mixed ferrosinels of the nickel–copper series and the cobalt–copper series are treated as solid solutions obtained by the substitution of nickel or cobalt of the simple ferrites with copper ions. In interpreting the XRD of such substitutions, the substitutional site can be considered as 'statistically' occupied, i.e., by a sort of 'composite atom' made up of the appropriate portions of the atoms involved [15]. There is a linear relation (Vegard's law) existing

between the lattice parameters and the composition of the solid solution [16]. Thus the pattern of the solid solution is expected to be intermediate between those of the pure substances. The fact that the mixed ferrites of both series give almost identical XRD patterns with those of NiFe₂O₄ or CoFe₂O₄ proves that the copper substitution does not change the site occupancy and that the mixed ferrites have the same inverse spinel structure as the pure ferrites. It is interesting to observe that the XRD data of all the samples are very much alike. In the present systems studied, the compositional differences are due to different proportions of the atoms nickel, cobalt or copper. These have close atomic numbers and hence close X-ray atomic scattering factors. Naturally, the lattice parameters are also expected to be very close to one another, as have been already reported [17]. The XRD patterns of sulphated samples did not show differences from those of the unmodified samples because of low sulphate loading.

3.1.2. Infrared spectra

The DRIFT and FT-IR spectra of the simple ferrites have been thoroughly discussed elsewhere [8]. The mixed ferrites too showed two strong bands around 700 and 500 cm⁻¹ in their DRIFT spectra, which were shown to be a common characteristic feature of ferrosinels [18]. Similarly sulphate loading has been qualitatively confirmed from the FT-IR spectra of the mixed ferrites, which always showed additional bands in the range 1200–1000 cm⁻¹ for the sulphated samples, but lacked the characteristic band near 1400 cm⁻¹ quoted as a common feature of all superacidic sulphated oxides [19]. The presence of this band and hence superacidity, depend very critically on the water content of the sulphated samples. In the present case, much of the characterisation and catalytic studies were done at the activation temperature of 300 °C, when the samples were still sufficiently hydrated. The TG results showed that the dehydration of the sulphated samples were delayed to a much higher temperature, just above 300 °C, than that for the unmodified ones. The TG–DTG curves for a typical sample are shown (Fig. 1).

3.1.3. BET surface area and EDX analysis

The surface area values of all the ferrosinels samples are given in Table 1. The data were reproducible within an error of 5%. These data show that

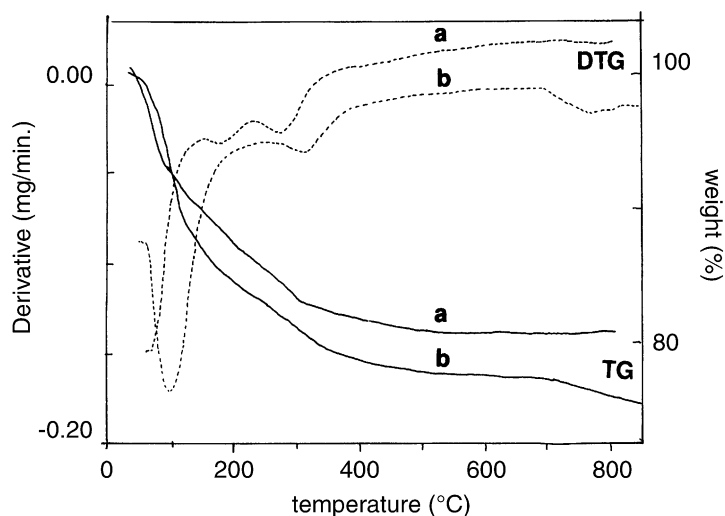


Fig. 1. TG–DTG curves for (a) NiFe_2O_4 and (b) $\text{SO}_4^{2-}/\text{NiFe}_2\text{O}_4$.

incorporation of copper into the ferros spinel systems of nickel and cobalt increases the surface area of the systems calcined at 300°C . This is a direct consequence of the fact, among the ferros spinels of nickel, cobalt and copper, copper ferrite has the highest surface area at 300°C . Surface areas of sulphated systems are invariably higher than those of the unmodified samples except for copper ferrite and cobalt–copper ferrite with $x = 0.7$. It has been shown that sulphation inhibits sintering of the metallic oxide and delays transformation from amorphous to crystalline phase [20]. Here also, the large surface areas of sulphated samples have been related to retardation of crystallisation

into the spinel phase. The chemical compositions of the samples were checked by EDX analysis and there was good agreement between the experimental values and those expected theoretically. The EDX analysis also showed that the sulphate loading on the samples were, on the average, to an extent of about 1% by mass of sulphur.

3.1.4. Mossbauer spectra

The Mossbauer parameters of the simple ferrites and a detailed discussion on their importance were given elsewhere [8]. The Mossbauer spectra of the mixed ferrites showed that the isomer shift (IS) values were

Table 1
Characterisation of the ferros spinel systems activated at 300°C

System	x	Surface area (m^2/g) ^a	Limiting amount of EA adsorbed ($\times 10^{-4}$ mmol/m^2) ^a		
			TCNQ	Chloranil	(TCNQ–chloranil)
$\text{Ni}_{1-x}\text{Cu}_x\text{Fe}_2\text{O}_4$	0.0	153 (196)	18.3 (8.9)	4.4 (3.0)	13.9 (5.9)
	0.3	177 (203)	16.7 (9.9)	6.0 (2.3)	10.7 (7.6)
	0.5	183 (211)	18.8 (8.6)	6.2 (1.5)	12.6 (7.1)
	0.7	174 (193)	18.0 (8.4)	6.5 (2.8)	11.5 (5.6)
	1.0	188 (188)	18.0 (9.3)	6.7 (3.4)	11.3 (5.9)
$\text{Co}_{1-x}\text{Cu}_x\text{Fe}_2\text{O}_4$	0.0	95 (107)	19.0 (5.7)	4.6 (1.0)	14.4 (4.7)
	0.3	137 (152)	19.2 (9.2)	5.2 (1.1)	14.0 (8.1)
	0.5	134 (155)	19.8 (8.1)	6.0 (0.7)	13.8 (7.4)
	0.7	167 (163)	16.6 (9.2)	6.1 (0.9)	10.5 (8.3)

^a Values for the sulphated samples are in parentheses.

in the range 0.3–0.4 mm/s with respect to natural iron, a value typical of Fe^{3+} with a total spin value of $\frac{5}{2}$. The quadrupolar splitting constant value (ΔE_Q) is a measure of the magnitude of electric field gradient (EFG) about the Mossbauer nucleus. ΔE_Q values for the copper containing spinels were found to be relatively larger. This is due to an additional distortion of charge symmetry caused by Jahn–Teller distortion. Although the ferrosinels are well known as ferrimagnetic materials, the expected magnetic hyperfine splitting was missing in the Mossbauer spectra. This has been attributed to the small particle size [21]. In order to check whether there is any change in the particle size or in the oxidation state of iron, the Mossbauer spectra of the samples were taken after these have been used for the vapour phase decomposition of CHOL at 300 °C. These spectra for cobalt ferrite and copper ferrite are given in Fig. 2 and the corresponding Mossbauer parameters are given in Table 2. The characteristic six line spectra representing the magnetic hyperfine interaction have been obtained. This shows the inherent ferrimagnetic nature of the spinel samples, which could be manifested by the growth in particle size during the catalytic reaction. The spectra (Fig. 2) consist of two separate six line patterns, one due to Fe^{3+} ions in the octahedral sites and the other due to the Fe^{3+} ions in the tetrahedral sites. As expected, when the magnetic interaction is operative, the quadrupolar interaction is very small and this explains the very small ΔE_Q values in the spectra shown.

3.2. Surface ED properties—evaluation of Lewis basicity

Surface ED properties which are measures of Lewis basicity have been investigated by adsorption of electron acceptors (EA) such as 7,7,8,8-tetracyanoquinodimethane (TCNQ), 2,3,5,6-tetrachloro-*p*-ben-

zoquinone (chloranil) and *p*-dinitrobenzene (PDNB) with electron affinity values of 2.84, 2.40 and 1.77 eV, respectively, in acetonitrile solution. The limiting amount of EA adsorbed has been estimated from the Langmuir plots. The data are given in Table 1. The values were reproducible within an error of 2%. The adsorption of PDNB was too little to be estimated. These data can give an idea on the strength and distribution of ED sites on the spinel surface. The limiting amount of EA adsorbed is higher for TCNQ than for chloranil as a result of the higher electron affinity value of TCNQ than that of chloranil. The limiting amount of TCNQ adsorbed gives a measure of strong as well as weak donor sites, whereas the values for chloranil give a measure of the strong and the moderately strong donor sites. The difference in the limiting amounts of TCNQ and chloranil adsorbed can give an idea of the number of weak donor sites.

Determination of acidic and basic sites on solid surfaces is a multifaceted problem and unfortunately there exists no general theory of the acidity or basicity of the solids that could serve as a basis for their determination. Transition metal oxides are generally categorised as acidic oxides although basic sites too exist on these. It will be interesting to analyse, in this context, the order of acidity/basicity among the octahedral cations of these ferrosinels on the basis of the usual theoretical parameters like charge to radius ratio, electronegativity, etc., of the cations. By such arguments, Fe^{3+} is the most acidic (least basic) while the order of acidity/basicity among Cu^{2+} , Co^{2+} and Ni^{2+} does not always correlate. This is due to the fact that the acido-basic properties of these ions are close to one another [8].

In agreement with the observation that copper ferrite has the highest proportion of the strong and the lowest proportion of the weak basic sites, the data in Table 1 show that copper doping in the mixed ferrites causes

Table 2
Mossbauer parameters of the magnetic hyperfine spectra of cobalt and copper ferrites

Sample	Site	IS (± 0.02 mm/s)	QS (± 0.02 mm/s)	Hn (± 5 kOe)	Line width (FWHM) (± 0.02 mm/s)
CoFe ₂ O ₄	A	0.06	0.03	487	0.55
	B	0.41	0.02	510	0.55
CuFe ₂ O ₄ (central doublet negligibly small)	A	0.18	−0.06	484	0.56
	B	0.34	0.05	514	0.56

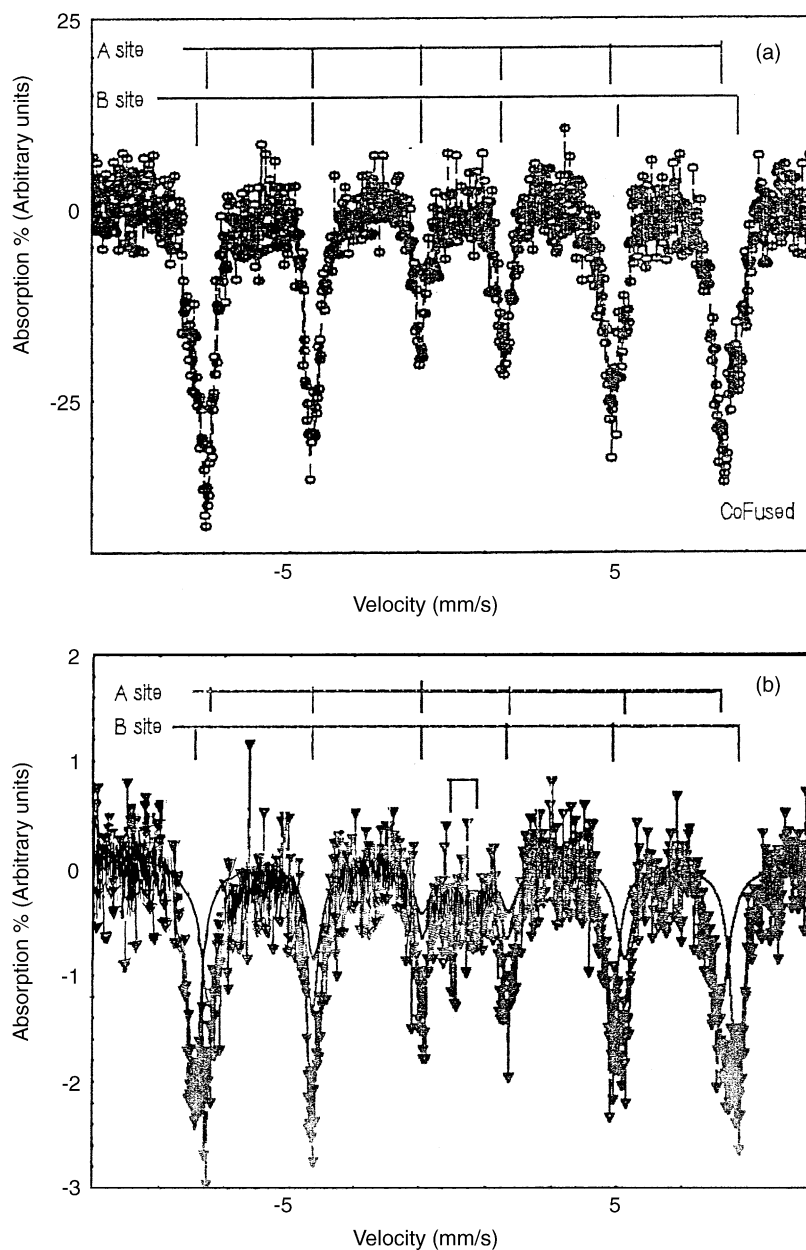


Fig. 2. The Mossbauer spectra showing magnetic hyperfine patterns: (a) CoFe_2O_4 ; (b) CuFe_2O_4 .

an increase in the strong basic sites and a decrease in the weak basic sites. In any case, sulphation causes a decrease in the strong as well as the weak basic sites. Sulphating agents being acidic, preferentially attack at the basic sites converting these to acidic sites.

3.3. Evaluation of surface acidity

Among the many methods adopted for assessing surface acidity of catalysts, TPD of basic probe molecules and calorimetric measurements have been

Table 3

Ammonia-TPD data on the ferrospinels, $A_{1-x}Cu_xFe_2O_4$ ($A = Ni$ or Co and $x = 0, 0.3, 0.5, 0.7$ and 1)^a, activated at 300 °C

System	x	Amount of ammonia desorbed at various temperatures ($\times 10^{-4}$ mmol m^{-2})						Total
		Weak ^b		Medium		Strong		
		100 °C	200 °C	300 °C	400 °C	500 °C	600 °C	
$Ni_{1-x}Cu_xFe_2O_4$	0.0	19.5 (16.9)	11.5 (9.7)	8.9 (7.7)	8.9 (6.8)	0.9 (5.8)	3.5 (3.1)	53.2 (50.0)
	0.3	4.9 (26.5)	5.6 (3.0)	3.5 (3.6)	2.1 (1.2)	0.7 (–) ^c	0.7 (–)	17.5 (34.3)
	0.5	4.1 (23.3)	4.7 (7.8)	4.7 (–)	3.4 (–)	2.7 (–)	1.3 (–)	20.9 (31.1)
	0.7	4.1 (31.1)	6.6 (6.8)	4.9 (1.9)	1.6 (–)	1.6 (–)	0.8 (–)	19.6 (39.8)
	1.0	13.4 (22.8)	8.7 (15.7)	2.0 (10.4)	1.3 (3.9)	Nil (1.9)	Nil (nil)	25.4 (54.7)
$Co_{1-x}Cu_xFe_2O_4$	0.0	12.8 (57.3)	10.4 (12.6)	9.2 (12.6)	5.2 (9.2)	3.9 (5.7)	2.6 (2.9)	44.1 (100)
	0.3	26.6 (34.3)	15.0 (28.5)	8.8 (19.2)	6.2 (9.6)	5.3 (7.9)	3.5 (2.4)	65.4 (102)
	0.5	12.4 (51.5)	8.6 (14.6)	5.7 (12.3)	4.8 (5.3)	2.9 (3.1)	1.9 (0.8)	36.3 (87.6)
	0.7	5.2 (29.3)	3.0 (12.4)	0.7 (7.1)	1.5 (4.4)	0.7 (2.6)	1.5 (nil)	12.6 (55.8)

^a Values for the sulphated samples are in parentheses.^b Ammonia desorbed at 100 °C contains some physisorbed ammonia too.^c (–) refers to negative values.

recommended as the most promising ones [50]. TPD of ammonia serves as a dependable technique for the determination of the number and distribution of acid sites. The results of ammonia-TPD are shown in Table 3. The data show that weak acid sites are the most abundant in the samples, followed by the medium strong sites while the number of strong acid sites are the least. The ammonia desorbed at 100 °C includes some physisorbed ammonia too, exaggerating the proportion of the weak sites. The data show that the total acidity and the medium strength acidity decrease in the order $Ni > Co \gg Cu$ among the simple ferrites and in the order $Co > Cu \cong Ni$ for their sulphated analogues. These results fairly agree with

those obtained from *n*-butylamine adsorption studies (Table 4).

Copper substitution into the ferrites causes a general decrease in their acidities which is more prominent with the Ni–Cu series than the Co–Cu series. Sulphation causes a tremendous increase in the acidities, especially of the weak and medium strong sites. The sulphated Ni–Cu series of ferrites seem to be chemically unstable during the ammonia-TPD as these give negative results during the volumetric estimation of desorbed ammonia at higher temperatures. Similar behaviour was observed by Lee and Park [51] who found that, after adsorption of ammonia, sulphated iron oxide was chemically unstable during heating.

Table 4

Comparison of acidity/basicity parameters obtained by the ‘direct’ method of *n*-butylamine adsorption/surface ED studies and the ‘indirect’ method of CHOL decomposition for simple ferrites

System	Acid sites <i>n</i> -butylamine adsorption (% weight loss, $\times 10^{-2}$ m^{-2})			Acidity parameter k_{CHENE} ($\times 10^{-4}$ h^{-1} m^{-2})	Basic sites limiting amount of ED adsorbed ($\times 10^{-4}$ mmol m^{-2})		Basicity parameter, k_{CHONE}/k_{CHENE}
	Weak	Medium	Strong		Weak	Medium + strong	
$NiFe_2O_4$	3.1	1.3	0.7	9.3	13.9	4.4	0.9
$CoFe_2O_4$	2.6	1.4	1.1	10.5	14.3	4.6	1.1
$CuFe_2O_4$	3.2	0.6	0.4	2.1	11.3	6.7	8.0
$NiFe_2O_4^a$	2.5	1.9	0.5	16.3	5.9	3.0	0.3
$CoFe_2O_4^a$	6.1	2.5	0.9	20.7	4.7	1.0	0.5
$CuFe_2O_4^a$	4.8	2.2	0.4	18.9	5.9	3.4	0.2

^a Sulphated samples.

It was suggested that ammonia preadsorbed on the sample reacted with the sulphate group upon heating and caused a change in the structure of surface sulphate, decomposing it and removing it at temperatures lower than those for thermal decomposition. Hence the ammonia-TPD results reflect the acidities of sulphated Ni–Cu series of ferrites erroneously.

DMP is a useful probe molecule for the selective determination of Brønsted acid sites because of the steric hindrance of the methyl groups [52]. Adsorption of DMP has been followed by TGA and the percentage weight loss per unit surface area was computed in three temperature ranges corresponding to weak, medium and strong acid sites. The results for a few samples are given in Table 6. The data show that the distribution of acid sites almost parallels with the trend shown by ammonia-TPD results. In other words, the main increase in acidity during sulphation is contributed by the weak and medium sites, proving that sulphation causes an increase in the Brønsted acid sites.

3.4. Vapour phase decomposition of CHOL

Decomposition of CHOL has been one of the most widely studied [13,14,22–25] model reactions to check the suitability of a catalyst for industry. Dehydration of CHOL gives cyclohexene (CHENE) while dehydrogenation gives cyclohexanone (CHONE). The CHENE activity is usually related to the surface acidity and the ratio of CHONE to CHENE activity is related to the surface basicity [24]. The catalyst samples

were activated in situ in air for 3 h before each experiment so as to get good reproducibility. The products were analysed by GC and the percentage yields of CHENE and CHONE were calculated from the % conversions and their selectivities. The minor products which included benzene and phenol were set aside under one banner as ‘other products’ in the calculation of selectivities. It is assumed that the dehydration and dehydrogenation processes represent a set of parallel reactions obeying first order kinetics. The integrated rate equation for a first order process in a flow system is similar to that in a static system provided the ‘time’ of the reaction is replaced by the ‘contact time’ [26]. Hence the intrinsic rate constant for each of CHENE and CHONE formation has been calculated.

3.4.1. Results

The percentage conversion, product selectivity and rate constants during CHOL decomposition over the various systems are given in Table 5. Reproducibility of these data were found to be within a maximum of 2%. The data of Table 5 enable us to draw the following conclusions:

- (i) Among the simple ferrites, the dehydration activity of the unmodified systems varies in the order $\text{Co} > \text{Ni} \gg \text{Cu}$ and of the sulphated systems in the order $\text{Co} > \text{Cu} > \text{Ni}$, whereas the dehydrogenation activity follows the order $\text{Cu} \gg \text{Co} > \text{Ni}$ for the unmodified systems and the order $\text{Co} > \text{Ni} > \text{Cu}$ for the sulphated samples.

Table 5

Decomposition of CHOL over the ferrites, $\text{A}_{1-x}\text{Cu}_x\text{Fe}_2\text{O}_4$ (A = Ni or Co and $x = 0, 0.3, 0.5, 0.7$ and 1)^a

Ferrite systems	x	% Conversion	Product selectivity (%)		Rate constant ($\times 10^{-4} \text{ h}^{-1} \text{ m}^{-2}$)		$k_{\text{CHENE}}/k_{\text{CHONE}}$
			CHENE	CHONE	k_{CHENE}	k_{CHONE}	
Simple: NiFe_2O_4	0.0	61 (94)	51 (61)	47 (26)	9.3 (16.4)	8.5 (5.5)	0.9 (0.3)
Simple: CoFe_2O_4	0.0	49 (72)	47 (62)	51 (38)	10.5 (20.7)	11.5 (11.3)	1.1 (0.5)
Simple: CuFe_2O_4	1.0	68 (76)	15 (80)	84 (18)	2.1 (18.9)	16.8 (2.9)	8.0 (0.2)
Mixed: Ni–Cu series	0.3	80 (84)	11 (17)	82 (80)	2.0 (2.9)	22.4 (20.9)	11.2 (7.2)
	0.5	71 (89)	13 (63)	83 (35)	2.0 (14.8)	18.4 (6.7)	9.4 (0.5)
	0.7	83 (85)	25 (77)	72 (21)	5.1 (20.8)	20.2 (3.9)	4.0 (0.2)
Co–Cu series	0.3	77 (55)	6 (47)	91 (52)	1.4 (7.3)	33.0 (8.3)	23.9 (1.1)
	0.5	79 (67)	9 (72)	89 (26)	2.1 (16.2)	34.2 (4.8)	16.0 (0.3)
	0.7	77 (47)	8 (60)	91 (38)	1.5 (7.8)	27.3 (4.6)	18.8 (0.6)

^a Values for the sulphated samples are in parentheses. Activation temperature of the catalyst, 300 °C; reaction temperature, 300 °C; amount of catalyst, 3 g; feed rate, 3.6 ml h⁻¹; contact time, 0.88 h; WHSV, 1.14 h⁻¹.

- (ii) Sulphation causes a noticeable enhancement in the dehydration activities of all the ferrites, this influence being maximum for copper ferrite and the least for nickel ferrite. This agrees with the acidity trends shown by ammonia-TPD results.
- (iii) The dehydration activities of all the copper containing mixed ferros spinels are monotonously much lower and the dehydrogenation activities are much larger than the corresponding values for the pure ferrites of nickel and cobalt.
- (iv) Except for nickel–copper ferrite with $x = 0.3$, sulphation of the mixed ferrites causes their dehydration activities to increase by many folds and their dehydrogenation activities to decrease by corresponding proportions.
- (v) There is no definite trend in the dehydration or dehydrogenation activities of all the samples that can be described as a function of copper concentration within the range $x = 0.3$ – 0.7 . The acidity/basicity data are too parallel with this aspect.
- (vi) On the average, the dehydrogenation activities and the $k_{\text{CHONE}}/k_{\text{CHENE}}$ ratios are much larger for the cobalt–copper series than for the nickel–copper series.
- (vii) The lower dehydrogenation activities of the sulphated samples are parallel with the lower limiting amount of EA adsorbed by the samples, as given in Table 1. Apart from this general trend, there is no one to one correspondence between the basicity parameters of CHOL decomposition and the same parameters in terms of limiting amount of EA adsorbed.
- (viii) The low dehydration activities of copper containing ferrites fairly agree with their low values of weak and medium strength acidities as shown by ammonia-TPD results.

3.4.2. Discussion

Selectivity in the alcohol decomposition reaction has long been regarded as one of the ‘indirect’ methods for investigating the acid–base properties of the catalytic sites of metal oxides. As first suggested by Ai [27] in the case of isopropanol decomposition and later confirmed by several authors [28–30], dehydration was catalysed by acid sites whereas the dehydrogenation was catalysed by both acid and basic sites through a concerted mechanism. As a consequence, the

dehydration rate could be regarded as a measure of the acidity of the catalyst, while the ratio of the dehydrogenation rate to the dehydration rate, as a rough index of the basicity of the catalyst. Thus, dehydration of CHOL leading to CHENE would be catalysed by acid centres, whereas its dehydrogenation leading to CHONE would be catalysed both by acid and basic sites.

The effect of sulphation on the selectivities gives a clue regarding the type of acid sites involved in the dehydration activity. We have already determined [8] the acidities of the simple ferros spinel systems by the ‘direct’ method of chemisorption of *n*-butylamine followed by gravimetric analysis of the desorbed probe molecules by TGA. The results of this analysis are reproduced along with the CHENE rate constants in Table 4.

From the data in Table 4, it is clear that sulphation of the ferrites has caused an increase in the number of weak and medium strong acid sites rather than that of strong acid sites. Creation of strong acid sites by sulphation depends on the nature of the oxide. In many cases, sulphation does not enhance reactivity catalysed by strong acid sites. Thus, Arata and Hino [31] observed that, for many metal oxides including NiO and CuO, there is little catalytic activity enhancement corresponding to strong acid sites, on sulphation. Miao et al. [32], during their study of sulphate-promoted mixed oxide superacids, found that addition of iron, nickel, cobalt, etc., to zirconia affected the catalytic activity only slightly.

Thus, in the present case, we can rule out the role of strong acid sites in deciding the dehydration activity because sulphation, while increasing the rate constants of dehydration, does not enhance the number of strong acid sites. On the contrary, we observe that the trends in the number of weak and moderately strong acid sites correlate fairly well with the dehydration activity. So we come to the conclusion that the weak to medium acid sites of the ferrite samples are more decisive in controlling the dehydration activities. Armendia et al. [33], during their investigation of different organic test reactions over acid–base catalysts, found that alcohol dehydration activity was appreciably correlated to Brønsted acidity and concluded that weak to medium acid sites were responsible for dehydration.

The increased dehydration activity of the sulphated samples can be explained as follows. First, sulphation

Table 6
Data of acidity measurement by gravimetric adsorption of DMP

Systems (activated at 300 °C)	% Weight loss ($\times 10^{-2} \text{ m}^{-2}$)			
	Weak (160–300 °C)	Medium (300–440 °C)	Strong (440–580 °C)	Total (160–580 °C)
CuFe ₂ O ₄	1.6	3.0	Nil	4.6
CuFe ₂ O ₄ ^a	1.4	4.7	0.1	6.2
Co _{0.5} Cu _{0.5} Fe ₂ O ₄	1.9	3.5	0.1	5.4
Co _{0.5} Cu _{0.5} Fe ₂ O ₄ ^a	3.2	3.9	0.2	7.3

^a Sulphated samples.

delays the transformation of substances from amorphous to crystalline phase [20]. Thus, at 300 °C, the sulphated ferrosin samples are much more hydroxylated than the unmodified ones. Hydroxyl groups can provide Brønsted acid sites and Lewis basic sites. So the increased acidity of medium strength, of sulphated samples is due to the increase in Brønsted acid sites which increase the dehydration activity. This had been supported by the DMP adsorption—TGA results (Table 6). Secondly, sulphating agents, being acidic species, preferentially attack the basic sites converting these to acidic sites. Both Lewis and Brønsted basic sites are present on the samples at 300 °C. At this temperature, the Lewis basic sites on metal oxides are mainly due to surface hydroxyl groups [34] and the Brønsted basic sites are due to coordinatively unsaturated oxide ions associated with neighbouring hydroxyl group. It was suggested [35] that the formation of acid sites during sulphation involved the chemical reaction between the surface hydroxyl groups of the metal hydroxide and the adsorbed H₂SO₄ (from the sulphating agent). Thus, sulphation preferentially occurs at the Lewis basic sites converting these to new Brønsted acid sites coming from the hydrogen sulphate group [36]. Hence the sulphated samples show very high dehydration and low dehydrogenation activities.

During their study of CHOL conversion at 300 °C, Martin and Duprez [24] noted that the presence of sulphate on zirconia increased its protonic acidity as proved by an increase in the CHENE activity. At the same time, sulphation on zirconia caused a decrease in the ratio of CHONE to CHENE activities. Bezouhanova and Al-Zihari [22] recommended the dehydration activity of CHOL conversion as a simple test to measure the Brønsted acid sites in a metal ox-

ide. The same opinion was also expressed by Martin and Duprez [24] and Armendia et al. [33]. A similar comparison can be made (Table 4) between the surface basicities determined earlier by adsorption of electron acceptors and the present basicity parameter, namely, $k_{\text{CHONE}}/k_{\text{CHENE}}$. During sulphation, some of the Lewis basic sites are converted to Brønsted acid sites as evident from decreased basicities of the sulphated samples. There is indeed a correlation between the (medium + strong) basicity parameters obtained from EA adsorption studies and the ratio of the rate constants during CHOL conversion, for the unmodified ferrites. There is no other correlation between the basicity parameters obtained by the two independent methods.

According to Armendia et al. [33], the widely documented correlation found for alcohol dehydration is not so clear for alcohol dehydrogenation. Gervasini and Auroux attempted to correlate the dehydration and dehydrogenation activities of isopropanol decomposition [37] with the acid–base character obtained by the calorimetric investigation [38] of a large series of metal oxides. They failed to get any simple relationship between the alcohol decomposition activities and acid–base properties and attributed the cause of this failure to the wide heterogeneity of the oxides chosen. The questionability regarding the use of alcohol decomposition activities as a measure of basicity seems to be applicable to our results also.

The unusual activities of copper containing ferrites, namely, a too low dehydration activity and a complementary leap in dehydrogenation activity, need further explanation. It is not by the low acidity or the high basicity of the samples alone. Other factors are suspected to be operative here.

Copper-based catalysts have attained considerable importance, owing to their selective properties in reactions involving hydrogen [39]. In their study of CHOL decomposition over various transition metal oxides, Bezouhanova and Al-Zihari [22] noted that ZnO and CuO were the most active materials for dehydrogenation. Present industrial practice of cyclohexanone manufacture, the key intermediate for nylon-6 or nylon-66, involves catalytic dehydrogenation of CHOL over commercial grade CuO/ZnO catalyst, known as Girdler-G-66B [40]. The double oxide system CuO/Cr₂O₃ supported on MgF₂ was found to be a very good catalyst for dehydrogenation of isopropanol and cumene [41]. Dehydrogenation activities of transition metal oxides are catalysed by basic as well as redox sites [41]. Isopropanol conversion is often sensitive to the redox properties of the catalysts [30,42,43]. Lahousse et al. [30] found that MgO (a very basic oxide) was totally inactive towards conversion of isopropanol to acetone, while a less basic ZnO was very active and concluded that dehydrogenation required redox sites rather than basic sites.

Among the dipositive cations in the ferrosinels systems under study, there is a wide difference in the redox properties of copper ion from those of Co²⁺ or Ni²⁺ ions. We propose that the unique behaviour of copper containing ferrites during CHOL decomposition is contributed by this difference in redox properties. Cu²⁺ with a higher electrode potential is more reducible and hence a more efficient oxidising agent than Ni²⁺ or Co²⁺ ions. The ferrosinels of nickel, cobalt and copper are n-type semiconductors with the bandgap or activation energy of 0.37 eV for NiFe₂O₄ [13], 0.52 eV for CoFe₂O₄ [12] and 0.19 eV for CuFe₂O₄ [44]. The very low activation energy for CuFe₂O₄ is a direct consequence of its increased reducibility and this makes the electron movements in the system easier, increasing its oxidation activity.

As the dehydration and dehydrogenation selectivities are complementary, a high dehydrogenation activity leads to a low dehydration activity. We have invoked the redox properties along with the basic properties to explain the high dehydrogenation activity of copper containing ferrites. Hence the complementary dehydration activity is reduced much lower than that demanded by the true acidity. The Mossbauer IS value (Table 2) of iron is still typical of Fe³⁺

proving that no bulk reduction has occurred during the reaction.

By oxygen-TPD technique, investigation of the oxygen uptake of 16 metal oxides including the first row transition metal oxides has been reported [45,46]. The authors found that the transition metal oxides always gave relatively large amounts of oxygen desorption even at high temperatures. CuO showed the largest amount of oxygen desorption, much larger than that shown by NiO, Co₃O₄ or Fe₂O₃. This property of CuO is expected to be retained in copper containing ferrosinels too. Sufficient amount of oxygen is adsorbed on the spinel during the activation stage in a current of dry air. This adsorbed oxygen can sustain the oxidation activity of copper containing ferrosinels without reducing these permanently.

The exact mechanism of gas phase dehydration of CHOL has proved difficult to study directly. But, by examining the dehydration of methyl substituted CHOLs, two possible mechanistic schemes have been proposed [47,48]. One of these is similar to E₂ elimination in which the catalyst provides both an acidic site to attack the hydroxyl group and a basic site to abstract a proton. The other is similar to E₁ elimination in which the reaction proceeds through the initial formation of a carbocation. Recently the mechanism of gas phase dehydration of CHOL has been thoroughly studied by Costa et al. [25] by means of deuterium labelling experiments and they could prove that the reaction indeed took place along the carbocation mechanism.

It is well known that the dehydrogenation catalysed by the acid–base sites takes place through a concerted mechanism in which the metal cation acts as a Lewis acid site accepting a hydride ion, whereas the oxygen anion acts as a Brønsted base accepting the proton of the alcohol group of CHOL [22,24,27,49]. In fact, the high oxidising ability of Cu²⁺ ion parallels with its strong Lewis acidity which enhances the dehydrogenation activity of copper containing ferrites.

The stability of the catalysts were tested by making the time on stream (TOS) studies under the experimental conditions of WHSV and reaction temperature over a period of 5 h. Most of the unmodified systems showed excellent stability (Fig. 3). Sulphate-modified systems showed decrease in activity with time. This is usually the case with sulphate-modified

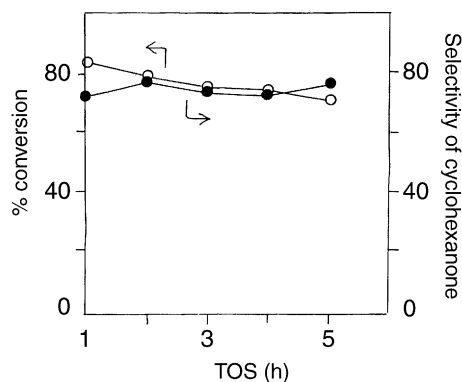


Fig. 3. Effect of TOS on CHOL decomposition over the catalyst, $\text{Ni}_{0.3}\text{Cu}_{0.7}\text{Fe}_2\text{O}_4$.

catalysts and is attributed to easy coke formation [20].

4. Conclusion

Preparation of ferrospinels of nickel, cobalt and copper by the room temperature coprecipitation method produced very fine particles with large surface areas. Sulphate modification has been done on all the catalytic systems and it very much enhanced the dehydration activity of all the samples during the decomposition of CHOL. The effect of copper substitution in the mixed ferrites was to increase the strong basic sites and decrease the weak basic sites with copper content. There was good correlation between the dehydration/dehydrogenation activities of CHOL decomposition and the acid–base parameters determined by the *n*-butylamine adsorption or ammonia-TPD/ED studies, in the case of simple ferrites. Copper containing ferrites showed very high activities for dehydrogenation and very low activities for dehydration, during CHOL decomposition. Along with the basic properties, the redox properties of copper ion are being suggested as the reason for this added dehydrogenation activity.

Acknowledgements

CGR thanks Dr. B.S. Rao and Dr. P.P. Bakare of the National Chemical Laboratory, Pune, for their help

and encouragement given to him.

References

- [1] J.P. Jacobs, A. Maltha, J.G.H. Reintjes, J. Drimal, V. Ponc, H.H. Brongersma, *J. Catal.* 147 (1994) 294.
- [2] J. Ziolkowski, Y. Barbaux, *J. Mol. Catal.* 67 (1991) 199.
- [3] P.S. Anilkumar, J.J. Shrotri, S.D. Kulkarni, C.E. Deshpande, S.K. Date, *Mater. Lett.* 27 (1996) 293.
- [4] K. Sreekumar, T.M. Jyothi, M.B. Talwar, B.P. Kiran, B.S. Rao, S. Sugunan, *J. Mol. Catal.* 152 (2000) 225.
- [5] K. Sreekumar, T. Mathew, S.P. Mirajkar, S. Sugunan, B.S. Rao, *Appl. Catal.* 201 (2000) L1.
- [6] K. Sreekumar, T.M. Jyothi, C.G. Ramankutty, B.S. Rao, S. Sugunan, *React. Kinet. Catal. Lett.* 70 (1) (2000) 161.
- [7] B.S. Rao, K. Sreekumar, T.M. Jyothi, Indian Patent No. 2707/98 (1998).
- [8] C.G. Ramankutty, S. Sugunan, *Appl. Catal. A* 218 (2001) 39.
- [9] C.S. Narasimhan, C.S. Swamy, *Appl. Catal.* 2 (1982) 315.
- [10] V. Krishnasamy, S. Chokkalingam, *J. Indian Chem. Soc.* 59 (1982) 641.
- [11] G.R. Dube, V.S. Darshane, *J. Chem. Soc., Faraday Trans.* 88 (9) (1992) 1299.
- [12] G.R. Dube, V.S. Darshane, *Bull. Chem. Soc. Jpn.* 64 (1991) 2449.
- [13] N.J. Jabarathinam, V. Krishnaswamy, in: P. Kanta Rao, R.S. Beniwal (Eds.), *Catalysis: Present and Future*, Publications and Information Directorate and Wiley Eastern Ltd., New Delhi, 1995, p. 288.
- [14] M.V. Joshi, S.G. Oak, V.S. Darshane, in: N.M. Gupta, D.K. Chakrabarty (Eds.), *Catalysis: Modern Trends*, Narosha, New Delhi, 1995, p. 275.
- [15] L.S. Dent Glasser, *Crystallography and Its Applications*, Van Nostrand Reinhold, New York, 1977, p. 114.
- [16] C. Whiston, in: F.E. Prichard (Ed.), *X-ray Methods*, Wiley, New York, 1991, p. 142.
- [17] G. Blasse, *Philips Res. Rep. Suppl.* 3 (1964) 22.
- [18] R.D. Waldron, *Phys. Rev.* 99 (1955) 1727.
- [19] M. Bensitel, O. Saur, J.C. Lavalley, B.A. Morrow, *Mater. Chem. Phys.* 19 (1988) 147.
- [20] X. Song, A. Sayari, *Catal. Rev.-Sci. Eng.* 38 (3) (1996) 329.
- [21] J.W. Niemantsverdriet, W.N. Delgass, *Top. Catal.* 8 (1999) 133.
- [22] C.P. Bezouhanova, M.A. Al-Zihari, *Catal. Lett.* 11 (1991) 245.
- [23] M. Dobrovolszky, P. Tetenyi, Z. Paal, *J. Catal.* 74 (1982) 31.
- [24] D. Martin, Duprez, *J. Mol. Catal.* 118 (1997) 113.
- [25] M.C.C. Costa, L.F. Hodson, R.A.W. Johnstone, J.Y. Liu, D. Whitaker, *J. Mol. Catal.* 142 (1999) 349.
- [26] K.J. Laidler, *Chemical Kinetics*, 3rd Edition, Harper, 1987, p. 33.
- [27] M. Ai, *J. Catal.* 40 (1975) 318.
- [28] P.E. Hathaway, M.E. Davis, *J. Catal.* 116 (1989) 279.
- [29] A.L. Mc Kenzie, C.T. Fishel, R.J. Davis, *J. Catal.* 138 (1992) 547.

- [30] C. Lahousse, J. Bachelier, J.C. Lavalley, H. Lauron-Pernot, A.M. Le Govic, *J. Mol. Catal.* 87 (1994) 329.
- [31] K. Arata, M. Hino, *Appl. Catal.* 59 (1990) 197.
- [32] C. Miao, W. Hua, J. Chen, Z. Gao, *Catal. Lett.* 37 (1996) 187.
- [33] M.A. Armendia, V. Borau, I.M. Garcia, C. Jimenez, A. Marinas, J.M. Marinas, A. Porras, F.J. Urbano, *Appl. Catal.* 184 (1999) 115.
- [34] K. Meguro, K. Esumi, *J. Adhes. Sci. Technol.* 4 (5) (1990) 393.
- [35] F.R. Chen, G. Coudurier, J.F. Joly, J.C. Vadrine, *J. Catal.* 143 (1993) 616.
- [36] O. Saur, M. Bensital, A.B.M. Saad, J.C. Lavalley, C.P. Tripp, B.A. Morrow, *J. Catal.* 99 (1986) 104.
- [37] A. Gervasini, A. Auroux, *J. Catal.* 131 (1991) 190.
- [38] A. Auroux, A. Gervasini, *J. Phys. Chem.* 94 (1990) 6371.
- [39] S. Berckman, C.J. Morrel, G. Egloff, *Catalysis: Organic and Inorganic*, Reinhold, New York, 1940.
- [40] W.S. Chen, M.D. Lee, *Appl. Catal.* 83 (1992) 201.
- [41] M. Wojciechowska, J. Haber, S. Lomnicki, J. Stoch, *J. Mol. Catal.* 141 (1999) 155.
- [42] M.I. Zaki, G.A.M. Hussein, H.A. El Ammany, S.A.A. Mansour, J. Polz, H. Knozinger, *J. Mol. Catal.* 57 (1990) 367.
- [43] L.J. Lakshmi, P. Kanta Rao, in: P. Kanta Rao, R.S. Beniwal (Eds.), *Catalysis: Present and Future*, Publication And Information Directorate/Wiley Eastern Ltd., New Delhi, 1995, p. 354.
- [44] S.P. Ghorpade, V.S. Darshane, S.G. Dixit, *Appl. Catal.* 166 (1998) 135.
- [45] M. Iwamoto, Y. Yoda, N. Yamazoe, T. Sieyama, *J. Phys. Chem.* 82 (1978) 2564.
- [46] J.L.G. Fierro, J.F. Garcia de la Branda, *Catal. Rev.-Sci. Eng.* 28 (2–3) (1986) 265.
- [47] J. Blanc, H. Pines, *J. Org. Chem.* 33 (1968) 2035.
- [48] C.L. Kibby, S.S. Lande, W.K. Hall, *J. Am. Chem. Soc.* 94 (1972) 214.
- [49] M. Ai, *Bull. Chem. Soc. Jpn.* 50 (1977) 2579.
- [50] J. Kijenski, A. Baiker, *Catal. Today* 5 (1989) 1.
- [51] J.S. Lee, D.S. Park, *J. Catal.* 120 (1989) 46.
- [52] A. Satsuma, Y. Kamiya, Y. Westi, T. Hattori, *Appl. Catal.* 194–195 (2000) 253.